

Kinetics of the borane reduction of pinacolone in THF catalyzed by two different oxazaboroles



Reinhard Schmidt,^{*a} Holger Jockel,^a Hans-Günther Schmalz^b and Helge Jope^b

^a Institut für Physikalische und Theoretische Chemie, J. W. Goethe-Universität, Marie-Curie-Str. 11, D60439 Frankfurt/M, Germany

^b Institut für Organische Chemie, Technische Universität Berlin, Straße des 17. Juni 135, D10623 Berlin, Germany

For the first time the kinetics of the borane reduction of a ketone catalyzed by oxazaboroles have been studied experimentally. Pinacolone (P) and $\text{BH}_3\text{-THF}$ are the reagents used, 1-phenyl-3,3-diethylperhydropyrrolo[1,2-*c*][1,3,2]oxazaborole **1a** and 1,3,3-triphenylperhydropyrrolo[1,2-*c*][1,3,2]oxazaborole **1b** the catalysts. The reaction of the ketone P with the oxazaborole–borane complex is the rate determining step of the catalytic cycle. The corresponding rate constant is about 40 times larger for **1b** than for **1a**. The presence of NaBH_4 , which is the stabilizer in commercial $\text{BH}_3\text{-THF}$ solutions, leads to a drastic acceleration of both the catalyzed and the direct borane reduction.

Introduction

The enantioselective borane reduction of ketones catalyzed by chiral oxazaboroles has generated great interest because of its many synthetic uses.^{1–5} Many different attempts have been made to further improve the enantioselectivity of the CBS (Corey–Bakshi–Shibata) reaction: variation of the catalyst,⁶ the borane reagent,⁷ the order and rate of addition,⁸ the solvent⁸ and the temperature.⁹ The principal mechanism of the catalyzed reaction seems to be understood as a result of experimental^{2,3,5,6,8,10,11} as well as on theoretical investigations.^{5,6,12–14} Nevertheless, considerable empirical fine tuning is still required to find optimum reaction conditions for high ee values. Kinetic investigations into the catalyzed reaction are required to address this unsatisfactory situation. Until now it has not been known which step of the assumed catalytic cycle is rate determining, nor how the reaction rate depends on the concentrations of borane and ketone, nor even how fast the catalyzed reaction, which has to compete with direct racemic borane reduction of ketones, proceeds.¹⁵ In order to obtain further insight into the CBS reduction, we set out to make the first detailed kinetic investigation. It has been shown by Corey *et al.*² that the ketone pinacolone (P) can be reduced with borane in tetrahydrofuran (THF) in the presence of the oxazaborole (OAB) 3,3-diphenylperhydropyrrolo[1,2-*c*][1,3,2]oxazaborole with high enantioselectivity (92% ee).² We used the OABs 1-phenyl-3,3-diethylperhydropyrrolo[1,2-*c*][1,3,2]oxazaborole **1a** and 1,3,3-triphenylperhydro[1,2-*c*][1,3,2]oxazaborole **1b** for the investigation of the kinetics of the catalyzed borane reduction of P in THF.

Results and discussion

Reactivity of the borane solutions

Borane exists in THF as a 1 : 1 $\text{BH}_3\text{-THF}$ complex (B–T).^{16,17} In our previous investigation of the direct borane reduction of P we observed very different reaction rates and kinetics, when using pure, freshly prepared, rather than commercial B–T as reducing agent.¹⁵ We showed that the stabilizer, NaBH_4 , present in the commercial reagent leads to a strongly enhanced reactivity. In order to determine whether the use of the different B–T reagents also leads to different kinetics of the catalyzed reaction, we have now performed experiments using OAB **1a** as catalyst (C). At overall concentrations of $[\text{B-T}]_0 = 0.23 \text{ mol dm}^{-3}$ and $[\text{C}]_0 = 0.012 \text{ mol dm}^{-3}$ we recorded very different kinetic curves

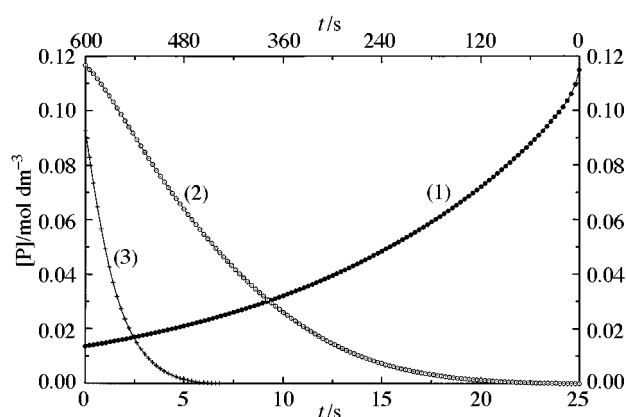


Fig. 1 Kinetic traces of the borane reduction of P catalyzed by OAB **1a** at 20 °C with $[\text{B-T}]_0 = 0.23 \text{ mol dm}^{-3}$, $[\text{C}]_0 = 0.012 \text{ mol dm}^{-3}$: (1) with freshly prepared pure B–T (upper timescale); (2) with commercial B–T (Aldrich) (lower timescale); and (3) with a freshly prepared B–T solution with $[\text{NaBH}_4]_0 \approx 0.01 \text{ mol dm}^{-3}$ (lower timescale)

of the consumption of P with (1) ‘self-prepared’ pure B–T,^{18,19} (2) commercial B–T, and (3) self-prepared B–T with added $[\text{NaBH}_4]_0 \approx 0.01 \text{ mol dm}^{-3}$. Fig. 1 illustrates the results. The time required for 50% conversion of the ketone decreases at 20 °C by more than two orders of magnitude in the series (1) $\tau_{1/2} = 200 \text{ s}$, (2) $\tau_{1/2} = 6 \text{ s}$ and (3) $\tau_{1/2} = 1 \text{ s}$. Thus, as in the case of the direct borane reduction of P, we find that the OAB catalyzed reaction occurs much faster with commercial B–T. Again we must conclude that it is the stabilizer, NaBH_4 , which enhances the reactivity of B–T.

Compared with the direct borane reduction of P we observe an increase in the reaction rate by a factor of about three in the presence of $0.012 \text{ mol dm}^{-3}$ OAB **1a** for ‘self-prepared’ pure B–T as well as for commercial B–T. From our earlier results on the direct borane reduction at 20 °C (reaction order in B–T $\text{RO} = 1$ with pure B–T, $\tau_{1/2} = 330 \text{ s}$ for $[\text{B-T}]_0 = 0.46 \text{ mol dm}^{-3}$; $\text{RO} = 1.6$ with commercial B–T, $\tau_{1/2} = 6 \text{ s}$ for $[\text{B-T}]_0 = 0.46 \text{ mol dm}^{-3}$)¹⁵ we calculate $\tau_{1/2} = 660 \text{ s}$ (pure B–T) and $\tau_{1/2} = 18 \text{ s}$ (commercial B–T) for the direct borane reduction with $[\text{B-T}]_0 = 0.23 \text{ mol dm}^{-3}$. The quantitative agreement of the catalytic acceleration by OAB **1a** for ‘self-prepared’ pure B–T as well as for commercial B–T could well be fortuitous. However, the comparison demonstrates that we also observe with the commercial reagent, whose reactivity is enhanced by NaBH_4 , an OAB

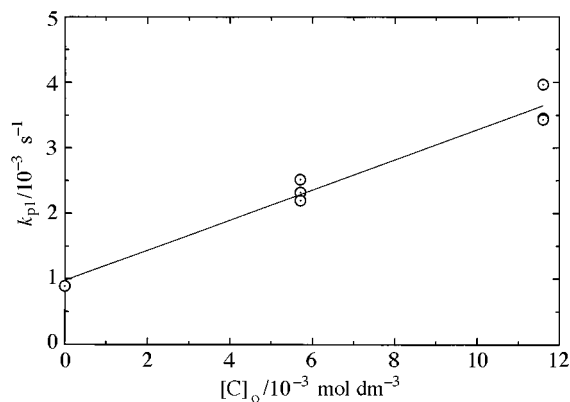


Fig. 2 Pseudo-first-order rate constants of the borane reduction of P catalyzed by OAB **1a** at 20 °C. $[B-T]_o = 0.26 \text{ mol dm}^{-3}$, $[P]_o = 0.080\text{--}0.120 \text{ mol dm}^{-3}$. $k_{p1} = k_d + k_c[C]_o$, $k_d = 0.00089 \text{ s}^{-1}$, $k_c = 0.23 \text{ dm}^3 \text{ mol}^{-1} \text{ s}^{-1}$.

induced catalysis. As mentioned by a referee, the enantioselectivity of the oxazaborole reaction should be conserved. In fact we also found large ee values with commercial B-T in preliminary experiments. In fact, the enantioselectivity of the catalytic reaction should only be dependent on the particular molecular structure of the catalyst–borane reagent adduct.

The nature of the reactive borane reagent in the commercial B-T is still unknown. Since the reactions become so fast in the presence of NaBH_4 that it becomes impossible to hold constant the temperature of the reaction system, as required for quantitative evaluation of the kinetic experiments, we have not yet been able to investigate in further detail the influence of NaBH_4 on the OAB catalyzed borane reduction of P.

Kinetics of the catalyzed reduction

In order to study the borane reduction catalyzed by OABs we decided to use 'self-prepared' pure B-T solutions in THF, and observed to a good approximation, first-order kinetics for P, see Fig. 1. Only if the reaction becomes very fast ($\tau_i \leq 50 \text{ s}$) and the initial concentration of pinacolone in the mixture is high ($[P]_i = [P]_o > 0.10 \text{ mol dm}^{-3}$) distinct deviations towards larger reaction rates are observed. In this case only the linear part of the plot $\ln[P]$ vs. time is used to evaluate the pseudo-first-order rate constants k_{p1} . The reason for the deviation is that the borane reduction of P is strongly exothermic. For example, in the presence of commercial $[B-T]_o = 0.46 \text{ mol dm}^{-3}$, when the reaction is catalyzed by NaBH_4 , the reaction of $[P]_o = 0.10 \text{ mol dm}^{-3}$ is complete within 20 s and leads to a temperature rise of the reaction solution of 5.6 °C. Of course, this causes an increase of the reaction rate. Since the reaction heat evolved is proportional to the concentration of P which has already reacted, the temperature rise becomes smaller for lower values of $[P]_o$ and for longer reaction times, in which the thermostat can remove the excess heat more efficiently.

If the temperature remains constant, the catalyzed reaction is first order in P. We have determined pseudo-first-order rate constants k_{p1} for the direct as well as the catalyzed borane reduction of P. The results obtained for OAB **1a** are presented in Fig. 2.

A linear correlation between k_{p1} and the overall catalyst concentration $[C]_o$ with a finite intercept is found. The experimental ordinate value of $k_{p1} = 0.00089 \text{ s}^{-1}$ is the overall pseudo-first-order rate constant k_d of the direct borane reduction, which is first order in B-T.¹⁵ The contribution of the catalytic reaction to the overall reaction increases linearly with $[C]_o$, indicating that direct and catalyzed borane reduction contribute additively to the overall reaction. The slope of the linear least squares fit can be considered as overall second-order rate constant, k_c , of catalysis [see eqn. (1)]. For OAB **1a** $k_c = 0.23 \pm 0.02 \text{ M}^{-1} \text{ s}^{-1}$ is

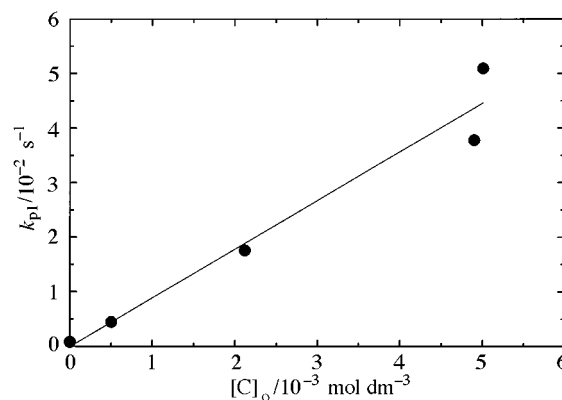


Fig. 3 Pseudo-first-order rate constants of the borane reduction of P catalyzed by OAB **1b** at 20 °C. $[B-T]_o = 0.227 \text{ mol dm}^{-3}$, $[P]_o = 0.080\text{--}0.140 \text{ mol dm}^{-3}$. $k_{p1} = k_d + k_c[C]_o$, $k_d = 0.00080 \text{ s}^{-1}$, $k_c = 9 \text{ dm}^3 \text{ mol}^{-1} \text{ s}^{-1}$.

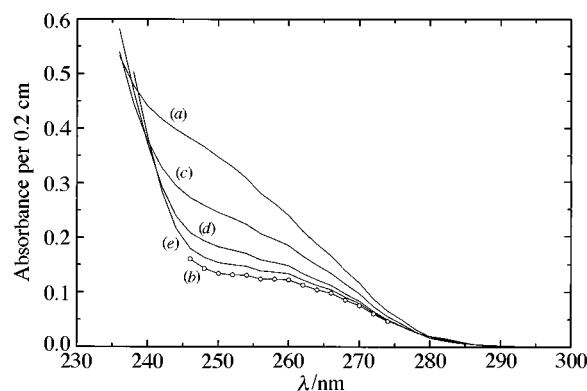


Fig. 4 Absorption spectra of (a) C and (b) borane adduct C-B for OAB **1b** and equilibrium spectra of mixtures of OAB **1b** with different overall concentrations of B-T. (c) $[B-T]_o = 0.047 \text{ M}$, $\tau_{\text{eq}} = 6 \text{ s}$, (d) $[B-T]_o = 0.25 \text{ M}$, $\tau_{\text{eq}} = 0.8 \text{ s}$, (e) $[B-T]_o = 0.50 \text{ M}$, $\tau_{\text{eq}} = 0.45$, where τ_{eq} is the time interval for arrival at equilibrium. For all spectra, $[C]_o = 5.0 \times 10^{-4} \text{ mol dm}^{-3}$.

$$k_{p1} = k_d + k_c[C]_o \quad (1)$$

obtained. Fig. 3 presents the corresponding plot for OAB **1b**, which differs only by the substituents R from OAB **1a**.

Again a linear correlation results, from which $k_c = 9 \pm 1 \text{ M}^{-1} \text{ s}^{-1}$ is calculated. Obviously, OAB **1b** is much the better catalyst for the reduction of P. We note a surprisingly strong substituent effect, causing a variation of k_c by a factor of 40 between the two catalysts. For OAB **1b** determinations of k_{p1} were performed at $[C]_o = 0.0050 \text{ mol dm}^{-3}$ and two different concentrations $[B-T]_o$. We found values of $k_{p1} = 0.05 \pm 0.01 \text{ s}^{-1}$ ($0.227 \text{ mol dm}^{-3}$) and $k_{p1} = 0.054 \pm 0.01 \text{ s}^{-1}$ (0.51 mol dm^{-3}), corresponding to rate constants k_c of 10 ± 2 and $11 \pm 2 \text{ M}^{-1} \text{ s}^{-1}$, respectively. These results indicate that k_c increases only slightly with $[B-T]_o$ in this concentration range.

Borane addition of the catalyst

Since the OABs catalyze the borane reduction of the ketone P, rapid reactions of C with P and/or B-T should occur. Preliminary experiments demonstrated that the reaction of OAB **1a** with P is very slow and occurs with half lifetime of about 4 h at 20 °C in THF. We can conclude therefore, that this reaction is not important in the catalytic reaction cycle and can be neglected. The reaction of both OABs with B-T, however, reaches equilibrium in a few seconds. Fig. 4 gives the absorption spectrum of OAB **1b** in THF and the equilibrium spectra obtained at $[C]_o = 5.0 \times 10^{-4} \text{ mol dm}^{-3}$ and different concentrations of B-T at 20 °C.

With increasing overall concentration $[B-T]_o$ the spectra become flatter and approach the product spectrum. Since the equilibrium spectra still change with the increase of $[B-T]_o$,

from 0.25 to 0.50 mol dm⁻³, the equilibrium must not be completely shifted to the product side at these concentrations, *i.e.* free catalyst is still present in these solutions.

Additionally, the time intervals τ_{eq} required for arrival at equilibrium are given in Fig. 4. The values of τ_{eq} are approximately reciprocally related to $[\text{B-T}]_0$. Since $[\text{B-T}]_0 \gg [\text{C}]_0$, this result demonstrates that we actually observe the equilibrium reaction $\text{C} + \text{B-T} \rightleftharpoons \text{C-B} + \text{T}$, where C-B stands for the borane adduct **2** of the oxazaborole catalyst and T for THF (see Scheme 1 showing the catalytic cycle). The lack of an isosbestic point at about 240 nm is presumably due to the presence of some impurity in the catalyst solution absorbing below 246 nm.

On the basis of the 1:1 reaction stoichiometry and the assumption that only C and C-B absorb in the wavelength range above 246 nm, where the solvent and B-T do not absorb,¹⁵ we calculate, with the solvent molarity $[\text{T}] = 12.3 \text{ mol dm}^{-3}$, the equilibrium constant $K = [\text{C-B}][\text{T}]/([\text{C}][\text{B-T}]) = 220 \pm 50$ for OAB **1b** at 20 °C. This value of K is very similar to the value $K = 260$, which was determined by Mathre *et al.*⁸ at 25 °C in THF by NMR measurements for 1-methyl-3,3-diphenylperhydropyrrolo[1,2-*c*][1,3,2]oxazaborole. This OAB differs from OAB **1b** only in its boron substituent. As a further result of the evaluation of spectra (a), (c)–(e) we obtain the absorption spectrum of the complex C-B **2** of OAB **1b**, which is given in Fig. 4.

The borane addition reaction of OAB **1b** was slow enough for $[\text{B-T}]_0 = 0.047 \text{ mol dm}^{-3}$ to be measured, time resolved, by spectrophotometry. As the overall concentration of catalyst of $[\text{C}]_0 = 5.0 \times 10^{-4} \text{ mol dm}^{-3}$ is much smaller than $[\text{B-T}]_0$ and $[\text{T}]$, forward and backward reaction of the borane addition to C are pseudo-first-order reactions with corresponding rate constants k_f and k_b . Assuming that only C and C-B absorb at the analysis wavelengths of 248 and 256 nm and using the formalism developed for the reactions close to the equilibrium state,²⁰ we evaluate k_b from eqns. (2) and (3) and from $k_f = k_b K [\text{B-T}]_0 / [\text{T}]$.

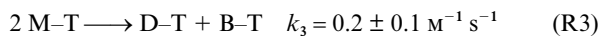
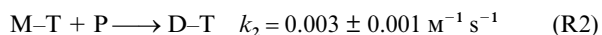
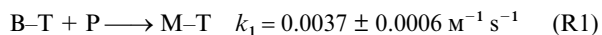
$$[\text{C}] = [\text{C}]_0 \{k_b + k_f \exp[-(k_f + k_b)t]\} / (k_f + k_b) \quad (2)$$

$$[\text{C-B}] = [\text{C}]_0 - [\text{C}] \quad (3)$$

We obtain $k_f = 0.34 \pm 0.07 \text{ s}^{-1}$ and $k_b = 0.40 \pm 0.12 \text{ s}^{-1}$ with OAB **1b**. Experiments performed under similar conditions with OAB **1a** revealed that the equilibrium reaction was too fast for a quantitative evaluation.

Simulation of the reaction by numerical integration

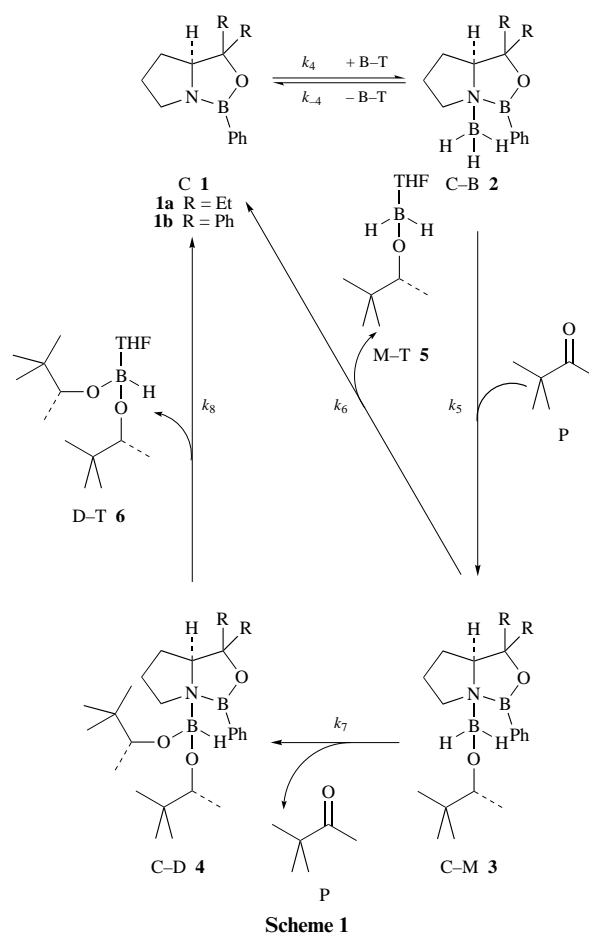
In our previous work on the kinetics of the direct borane reduction we demonstrated that the three reactions (R1) to (R3), with



corresponding rate constants k_1 to k_3 (20 °C), are sufficient for a simulation of the experimental kinetic curves by numerical integration.¹⁵ M-T represents the monoalkoxyborane-THF complex derived from P [M = 2-*tert*-butylethoxyborane] and D-T is the corresponding dialkoxyborane complex. Dialkoxyboranes are the only reaction products formed in the direct borane reduction of ketones.^{21,22} For the borane reduction catalyzed by OABs it has also been shown that only two moles of ketone are reduced by one mole of C-B.⁸

In Scheme 1 we present a simplified catalytic cycle for the CBS reduction, which considers the results of experimental and theoretical studies.

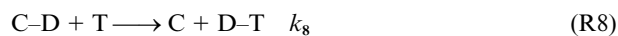
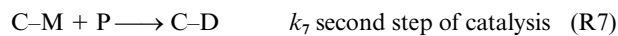
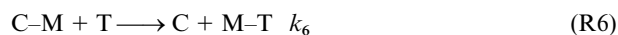
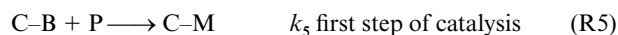
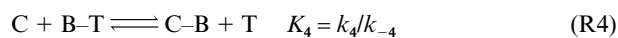
The reversible addition of borane to the catalyst **C 1** forms the complex C-B **2**. It has been shown by NMR spectroscopy



Scheme 1

of solutions of C-B in THF³ and by single-crystal X-ray spectroscopy of solid C-B^{8,11} that BH₃ is coordinated to the nitrogen atom of the OAB ring in C-B. Since the lone pair electrons of the nitrogen can no longer be shared with the boron atom of the heterocycle, the acidity of the boron atom of the OAB ring is distinctly increased in C-B relative to C. The ketone P couples with the oxygen to the electrophilic ring-boron of C-B to form a ternary complex. It is generally accepted that hydride transfer occurs from the NBH₂ unit to the carbonyl carbon *via* a six-membered cyclic transition state. The intermediate rearranges to yield the monoalkoxyborane adduct C-M of the oxazaborolidine catalyst.^{5,12} AM1 semiempirical MO calculations¹⁴ and low temperature (–100 °C) NMR spectroscopy in CD₂Cl₂¹⁰ yielded a tricyclic structure for C-M, in which the oxygen atom of the alkoxy group is bound to both the boron atom of the NBH₂ group and the boron atom of the oxazaborole ring, forming a four-membered ring with the atom sequence –O–B–N–B–. However, we assume for the product complex C-M in THF at room temperature structure **3**, which is very similar to the structure **2** of complex C-B, since we observe only very minor spectral changes in the reaction spectra of the whole catalytic cycle, *vide infra*. We therefore expect the electronic structures of the different product complexes C-M and C-D of the catalyst and of the borane adduct C-B **2** to be very similar. This certainly holds true for the structures **3** and **4** of Scheme 1, but would be less so for the alternative tricyclic structure discussed above. However, the formal kinetics developed below hold true regardless of the actual structure of the product complexes of the catalyst. C-M reacts in Scheme 1 with T and dissociates into C and M-T **5** in a reaction very similar to the backward reaction of the borane addition equilibrium of the catalyst. In competition with its dissociation, the complex C-M can add and reduce a second ketone molecule and yield the dialkoxyborane adduct C-D **4** in a reaction sequence very similar to the first step of the catalytic cycle.

Finally, C–D reacts with T and dissociates into C and D–T **6**. Thus, in addition to the three reactions of the direct borane reduction, reactions (R4) and (R8) have to be considered in a quantitative description of the kinetics.



Eqns. (4) to (11) give the derivatives with respect to time of the concentrations of the different species.

$$d[B-T]/dt = -(k_1[P] + k_4[C])[B-T] + k_3[M-T]^2 + k_{-4}[C-B][T] \quad (4)$$

$$d[P]/dt = -(k_1[B-T] + k_2[M-T] + k_5[C-B] + k_7[C-M])[P] \quad (5)$$

$$d[M-T]/dt = k_1[P][B-T] + k_6[C-M][T] - k_2[P][M-T] - 2k_3[M-T]^2 \quad (6)$$

$$d[D-T]/dt = k_2[P][M-T] + k_3[M-T]^2 + k_8[C-D][T] \quad (7)$$

$$d[C]/dt = -k_4[B-T][C] + (k_{-4}[C-B] + k_6[C-M] + k_8[C-D])[T] \quad (8)$$

$$d[C-B]/dt = k_4[B-T][C] - [C-B](k_{-4}[T] + k_5[P]) \quad (9)$$

$$d[C-M]/dt = k_5[P][C-B] - [C-M](k_6[T] + k_7[P]) \quad (10)$$

$$d[C-D]/dt = k_7[P][C-M] - k_8[C-D][T] \quad (11)$$

Besides k_1 , k_2 and k_3 we already know $K_4 = K = 220$, $k_4 = k_f/0.047 = 7.2 \text{ M}^{-1} \text{ s}^{-1}$ and $k_{-4} = k_b/12.3 = 0.033 \text{ M}^{-1} \text{ s}^{-1}$. However, four further rate constants still have to be determined in numerical fits to the experimental kinetic runs, which have been performed in dependence of the borane, catalyst and ketone concentrations. Solutions containing equilibrium mixtures of borane and catalyst in THF were mixed with solutions of P in THF. The respective overall concentrations in the reaction mixtures are $[B-T]_0$, $[C]_0$ and $[P]_0$. At time zero of the reaction the following initial concentrations hold true in the reaction mixture: $[P]_i = [P]_0$, $[M-T]_i = 0$, $[D-T]_i = 0$, $[C-M]_i = 0$, $[C-D]_i = 0$. Besides C the complex C–B is present from the beginning, on leading to $[B-T]_i < [B-T]_0$ and $[C]_i \ll [C]_0$. $[B-T]_i$, $[C]_i$ and $[C-B]_i$ can be calculated using the equilibrium constant K_4 . As $[B-T]_0 \gg [C]_0$ is always given, eqns. (12) to (14) hold approximatively true at $t = 0$.

$$[B-T]_i = [B-T]_0 - [C]_0(K_4/[T])/[1 + (K_4/[T])[B-T]_0] \quad (12)$$

$$[C]_i = [C]_0/[1 + (K_4/[T])[B-T]_0] \quad (13)$$

$$[C-B]_i = [C]_0 - [C]_i \quad (14)$$

The balance equations (15) to (17) relate $[B-T]_0$, $[P]_0$ and $[C]_0$.

$$[B-T]_0 = [B-T] + [M-T] + [D-T] + [C-B] + [C-M] + [C-D] \quad (15)$$

$$[P]_0 = [P] + [M-T] + 2[D-T] + [C-M] + 2[C-D] \quad (16)$$

Table 1 Rate constants k_5 to k_8 of the catalytic cycle obtained by numerical integration (20 °C); C = OAB **1b**. $k_1 = 0.0037$, $k_2 = 0.003$, $k_3 = 0.2$, $k_4 = 7.2$ and $k_{-4} = 0.033$ (all in $\text{M}^{-1} \text{ s}^{-1}$) are fixed parameters.

	$k_5/\text{M}^{-1} \text{ s}^{-1}$	$k_6/\text{M}^{-1} \text{ s}^{-1}$	$k_7/\text{M}^{-1} \text{ s}^{-1}$	$k_8/\text{M}^{-1} \text{ s}^{-1}$
1	15 ± 2.5	0.7 ± 0.2	0	0
2	13 ± 1.5	0	10 ± 3	0.65 ± 0.13
3	14 ± 2	0.23 ± 0.04	9 ± 3.5	0.65 ± 0.13

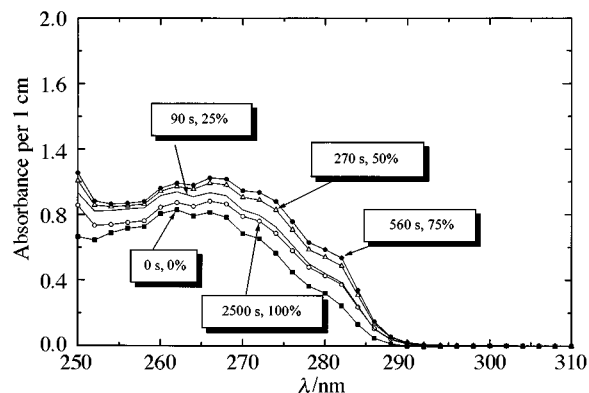


Fig. 5 Corrected reaction spectra of the borane reduction of P catalyzed by OAB **1a** at selected conversions of P (%) and corresponding times of reaction (s). The absorption of P has been subtracted from the overall reaction spectra to obtain the corrected reaction spectra. $[P]_0 = 0.08$, $[B-T]_0 = 0.23$, $[C]_0 = 0.0057 \text{ mol dm}^{-3}$. (■) 0% conversion, 0 s reaction time; (—) 25%, 90 s; (△) 50%, 270 s; (●) 75%, 560 s; (○) 100%, 2500 s.

$$[C]_0 = [C] + [C-B] + [C-M] + [C-D] \quad (17)$$

at any time during the reaction with the concentrations of the different species present in the reaction mixture derived from borane, pinacolone and catalyst. Since $[T] \gg [B-T]_0$, $[T] = 12.3 \text{ mol dm}^{-3}$ is set constant. The system of differential equations (4) to (11) has been solved by numerical integration using eqns. (12) to (17). The whole experimental kinetic curves with catalyst **1b** can be reproduced by three different sets of rate constants given in Table 1.

Obviously, the number of variables is too large for a definite numerical solution of the problem. We can, however, distinguish between the following situations (see also Scheme 1): (1) k_7 and k_8 are zero. Then, the reaction of C–B **2** proceeds only to C–M **3**, which subsequently reacts with T to form C **1** and M–T **5**. C–B is regenerated by reaction of C with B–T. This is a small catalytic cycle with three linearly independent reactions [(R4) to (R6)] in which only one ketone molecule is reduced. (2) k_6 is zero, C–B **2** reacts sequentially with two ketone molecules to give C–D **4**, which further reacts with T to yield C and D–T **6**. This is a large catalytic cycle with four linearly independent reactions [(R4), (R5), (R7) and (R8)]. (3) None of the rate constants is zero, all five linearly independent reactions (R4) to (R8) take place.

The analysis of reaction spectra by means of extinction difference quotient (EDQ) diagrams allows us to obtain information about the number of linearly independent reactions.²³ For example, if a reaction leads to curved EDQ2 diagrams but to linear EDQ3 diagrams, three linearly independent reactions must be taking place.²³ Since the absorption of P dominates the reaction spectra, it is useful to subtract the ketone absorbance from the reaction spectra before doing the analysis. Fig. 5 shows such corrected reaction spectra at selected conversions of the ketone with the corresponding reaction times.

At time zero we observe a spectrum with maximum absorption at 262 nm, which is composed mainly of the absorption spectrum of C–B and only to a lesser extent the spectrum of C. The band increases rapidly and shifts slightly to the red with

Table 2 Rate constants (20 °C) and activation parameters of the direct and the catalyzed borane reduction of pinacolone

	$k/\text{M}^{-1} \text{s}^{-1}$	$\Delta G^\ddagger/\text{kJ mol}^{-1}$	$\Delta H^\ddagger/\text{kJ mol}^{-1}$	$\Delta S^\ddagger/\text{kJ mol}^{-1} \text{K}^{-1}$
Direct	0.0037 ± 0.0006	93.2 ± 0.4	52 ± 6	-0.14 ± 0.02
OAB 1a	0.23 ± 0.02	83.1 ± 0.2	33 ± 6	-0.17 ± 0.02
OAB 1b	9.0 ± 1.0	74.2 ± 0.3	24 ± 5	-0.17 ± 0.02

increasing conversion of P. At 75% conversion the maximum absorbance is reached and the band decreases again without reaching the starting spectrum. These small spectral changes must be caused by production of UV absorbing products besides C and C–B, namely C–M and C–D. Since we observe only small spectral changes, the variously complexed catalyst molecules are presumably very similar in electronic structure to C–B and are most probably the alkoxyborane complexes with structures **3** and **4** of Scheme 1.

The analysis of the corrected reaction spectra, taken at constant time intervals of 10 s, results in curved EDQ2 and EDQ3 diagrams, demonstrating that there are more than three linearly independent reactions in the catalytic cycle, in which C, C–B, C–M and C–D take part. Thus, we exclude experimentally the small catalytic cycle (1) (k_7 and k_8 are zero, above). This result is in agreement with the observation that two moles of ketone are reduced by one mole of C–B.⁸ The small catalytic cycle allows only a 1 : 1 stoichiometry. Both alternatives (2) and (3) demand the reactions $\text{C–B} + \text{T} \longrightarrow \text{C} + \text{B–T}$ and $\text{C–D} + \text{T} \longrightarrow \text{C} + \text{D–T}$. If these reactions take place, the closely related reaction $\text{C–M} + \text{T} \longrightarrow \text{C} + \text{M–T}$ cannot be forbidden, as assumed in alternative (2). It seems that only the complex situation described by alternative (3) is realistic.

It is interesting to compare the values of the rate constants of the different reactions. Steric effects are observed. The size of the complexes increases in the series C–B, C–M, C–D. In the same series we observe strongly increasing rate constants for the corresponding dissociation reactions: $k_{-4} = 0.033 \text{ M}^{-1} \text{ s}^{-1}$, $k_6 = 0.23 \text{ M}^{-1} \text{ s}^{-1}$ and $k_8 = 0.65 \text{ M}^{-1} \text{ s}^{-1}$. This result can be explained by the increase in steric crowding in the series of OAB–borane complexes. Both catalytic steps, which are very similar reactions, have large rate constants of $k_5 = 14 \text{ M}^{-1} \text{ s}^{-1}$ and $k_7 = 9 \text{ M}^{-1} \text{ s}^{-1}$, whereby the reaction of the ketone molecule with the smaller complex (C–B) occurs with the larger rate constant, which we interpret again as the consequence of a steric effect. The addition reactions of M–T or D–T with C to form C–M or C–D have not explicitly been considered in the kinetic evaluation. This seems justified, since the respective equilibrium constants are certainly much smaller than K_4 because of the larger steric crowding in the complexes C–M and C–B. Therefore, and because of the comparatively low concentrations of M–T and D–T, the respective equilibria are probably shifted far to the catalyst side.

The rate determining step of the catalytic cycle

The investigation of the data sheets of the numerical integration demonstrates that $[\text{C–T}] > [\text{C–M}]$, which is in accordance with the assumption of reaction (R5) as rate determining step. If we apply the Bodenstein hypothesis to C–M, we obtain eqn. (18) for the reaction rate. Experimentally, we found that the

$$-\text{d}[\text{P}]/\text{dt} = k_5[\text{P}][\text{C–B}] \\ = k_5[\text{P}][\text{C}]_0(K_4/[\text{T}])[\text{B–T}]/\{1 + (K_4/[\text{T}])[\text{B–T}]\} \quad (18)$$

reaction rate is a good approximation to that given by $-\text{d}[\text{P}]/\text{dt} = k_c[\text{P}][\text{C}]_0$. By comparison we obtain eqn. (19), which

$$k_c = k_5(K_4/[\text{T}])[\text{B–T}]/\{1 + (K_4/[\text{T}])[\text{B–T}]\} \quad (19)$$

demonstrates that $k_c = k_5$ as long as $(K_4/[\text{T}])[\text{B–T}] \gg 1$. For OAB **1b** we determined at $[\text{C}]_0 = 0.0050 \text{ mol dm}^{-3}$ values of k_c

for two different concentrations $[\text{B–T}]_0$: $k_c = 10 \pm 2 \text{ M}^{-1} \text{ s}^{-1}$ ($0.227 \text{ mol dm}^{-3}$) and $k_c = 11 \pm 2 \text{ M}^{-1} \text{ s}^{-1}$ (0.51 mol dm^{-3}), *vide supra*. Taking the data of k_5 and $K_4/[\text{T}]$ obtained in this study we calculate from eqn. (19) $k_c = 11.2 \text{ M}^{-1} \text{ s}^{-1}$ ($0.227 \text{ mol dm}^{-3}$) and $k_c = 12.6 \text{ M}^{-1} \text{ s}^{-1}$ (0.51 mol dm^{-3}), which are in fair agreement with these experimental values. If we consider that, because of the consumption of borane during the reaction, the average concentration of B–T is smaller than given by $[\text{B–T}]_0$, the agreement of experimental values of k_c and those calculated by eqn. (19) becomes even better. This confirms that reaction (R5) is indeed the rate determining step of the catalytic reaction with OAB **1b**. It is assumed that this holds true also for OAB **1a**.

Activation parameters

Temperature dependent determinations of k_c have been performed in the range 10 to 30 °C with both OABs. The activation parameters, which refer to the reaction $\text{C–B} + \text{P} \longrightarrow \text{C–M}$ and the corresponding rate constants are listed in Table 2. In addition, the respective parameters for the reaction $\text{B–T} + \text{P} \longrightarrow \text{M–T}$, the initial step of the direct borane reduction, are given.¹⁵ The comparison demonstrates that at 20 °C the rate constant increases by factors of 70 (OAB **1a**) or 2700 (OAB **1b**) going from the direct to the catalyzed reactions. The activation entropies ΔS^\ddagger are the same for both catalysts. This is not surprising, since both differ only with respect to the substituents R. The change in the degree of order of the system between transition state and educts should be the same for OAB **1a** and OAB **1b** as the different substituents R are far apart from the reaction center. The values of ΔS^\ddagger are more negative for the catalyzed reactions than for the direct reaction. This result is also as one would expect as the addition of P to C–B and the subsequent stereoselective hydride shift imposes greater steric demands to reach the transition state than does the nonstereoselective reaction of P with B–T. More negative values of ΔS^\ddagger usually result in larger positive contributions to the free activation enthalpy and consequently in smaller rate constants. Nevertheless, for both catalysts rate constants k_c are much larger than the rate constant of the direct borane reduction because of the smaller activation enthalpies ΔH^\ddagger of the catalyzed reactions [by 19 (OAB **1a**) and 28 kJ mol^{-1} (OAB **1b**)]. It is interesting to note that the 40-fold larger value of k_c of OAB **1b** compared with OAB **1a** is exclusively due to a smaller value of ΔH^\ddagger (by 9 kJ mol^{-1}). The discussion of the possible reasons for the substituent effect on k_c still seems premature, as rate constants and activation parameters have only been determined for two catalysts.

A comparison of the experimentally-obtained activation enthalpies with values of ΔH^\ddagger resulting from theoretical calculations is difficult. Unfortunately, only OABs of different structure or with different substituents to those in our experiments have been theoretically investigated. Different substitution, however, can lead to distinctly different activation enthalpies, as we have observed experimentally. It was found by Quallich *et al.*⁶ that *ab initio* molecular orbital calculations resulted in values of ΔH^\ddagger that vary considerably with the level of theory. Moreover, the existence of key intermediates was found to depend on the level of theory employed. Apparently better results have been obtained by Linney *et al.*¹⁴ using semiempirical molecular orbital calculations with AM1 parametrization. They investigated the direct borane reduction of propanone as well as the borane reduction catalyzed by an OAB, which differs

from OAB **1a** by R = H and by Me substitution rather than Ph of the boron. $\Delta H^\ddagger = 84 \text{ kJ mol}^{-1}$ was obtained for the direct borane reduction of propanone by B–T, a distinctly larger value than $\Delta H^\ddagger = 52 \text{ kJ mol}^{-1}$ determined by us for pinacolone. ΔH^\ddagger was calculated to be about 45 kJ mol^{-1} lower for the catalyzed process than for the direct borane reduction. This difference is again larger than the corresponding experimental results of 19 kJ mol^{-1} (OAB **1a**) and of 28 kJ mol^{-1} (OAB **1b**). It would be very interesting to see whether AM1 calculations with catalysts **1a** and **1b** and with ketone P would possibly result in a closer agreement with the experiments.

Conclusions

The borane reduction of ketones catalyzed by oxazaboroles competes with the direct borane reduction. The rate determining step of the catalyzed reaction is the formation of the monoalkoxyborane adduct of the oxazaborole, by the reaction of the ketone with the oxazaborole–borane complex. A large catalytic cycle is operating with two subsequent addition–reduction steps and with an additional short-cut branch from the complex monoalkoxyborane–catalyst to the catalyst.

Experimental

Techniques

Melting points were measured with a Büchi 510 apparatus and are uncorrected. FT-infrared spectra were recorded with a Nicolet Magna FT-IR spectrometer. ^1H NMR and ^{13}C NMR spectra were recorded on a Bruker AM 270 spectrometer. Chemical shifts are reported in ppm and were referenced to the residual CHCl_3 resonances ($7.26 \text{ ppm}/77.00 \text{ ppm}$). J values are given in Hz. Elemental analyses were obtained with a Perkin-Elmer CHNO/S-Analysator 2400 II or a Heraeus CHN-Rapid. Optical rotations were measured at 20°C in CHCl_3 on a Perkin-Elmer 241 polarimeter. The reactions were followed spectrophotometrically using a stopped-flow apparatus and a computerized Hewlett-Packard HP8452A diode array spectrophotometer as described earlier.¹⁵ The handling of the materials and the preparation of the solutions was done under Ar to avoid contamination by water. Unless otherwise stated, all kinetic experiments were carried out at 20°C .

Preparations

(S)-(–)-2-[Hydroxy(diphenyl)methyl]pyrrolidine. This was obtained using a modified literature procedure;²⁵ colorless crystals from *n*-heptane; mp 79°C (lit., $74\text{--}74.8$,² $79\text{--}79.5^\circ\text{C}^{25}$); $[\alpha]_{589} = -67.3^\circ$, $c = 2.0$ (lit.,² $[\alpha]_{589} = -68.1^\circ$, $c = 3.17$ in CHCl_3).

(S)-(–)-2-(1-Hydroxy-1-ethylpropyl)pyrrolidine. To a solution of 20.1 g (81.3 mmol) of **(S)-(–)-1-benzyl-2-(1-hydroxy-1-ethylpropyl)pyrrolidine** (obtained from L-proline according to the procedure of Enders²⁴) in 180 ml of MeOH was added 1 g of 10% Pd(OH)₂ on carbon (Degussa) and 2.5 ml of AcOH. The mixture was then stirred in a hydrogen atmosphere (1.1 atm) for 18 h , filtered through a short pad of Celite and concentrated *in vacuo*. The residue was partitioned between 60 ml of 1 M NaOH and 60 ml of CHCl_3 and the aqueous layer extracted several times with CHCl_3 . The combined organic layers were washed with brine, dried (MgSO_4) and concentrated *in vacuo*. Kugelrohr distillation (60°C , 0.5 mbar) finally gave the product in 75% yield as colourless needles, mp $48\text{--}49^\circ\text{C}$; $[\alpha]_{589} = -36.9^\circ$, $c = 2.0$; $\nu_{\text{max}}(\text{CCl}_4)/\text{cm}^{-1}$ $3500\text{--}3400$, 3379 , 2968 , 2942 , 2881 , 1460 , 1400 , 1137 ; $\delta_{\text{H}}(\text{CDCl}_3, 270 \text{ MHz})$ 3.1 (Ψt , J 8 , 1H), $2.98\text{--}2.87$ (m, 2H), $1.8\text{--}1.6$ (m, 4H), $1.60\text{--}1.32$ (m, 4H), 0.86 (Ψt , J 7.5 , 6H); $\delta_{\text{C}}(\text{CDCl}_3, 270 \text{ MHz})$ 73.8 , 63.3 , 45.6 , 29.5 , 26.7 , 26.2 , 25.2 , 8.0 , 7.8 ; Anal. Calc. for $\text{C}_9\text{H}_{19}\text{NO}$: C, 68.74 ; H, 12.18 ; N, 8.91 . Found: C, 68.58 ; H, 12.18 ; N, 8.83% .

Preparation of the oxazaborole catalysts 1a and 1b.²⁵ In a dry 100 ml Schlenk-flask 2.0 mmol of the amino alcohol and 2.1 mmol of phenylboronic acid were suspended in 40 ml of dry toluene. The mixture was heated to reflux in an atmosphere of argon for 24 h with azeotropic removal of water, which was trapped by 10 g of 4 \AA molecular sieves placed in a pressure equalizing dropping funnel between the flask and the condenser. The toluene was then removed *in vacuo* and the residue purified by Kugelrohr distillation ($115\text{--}120^\circ\text{C}$, 0.5 mbar for **1a** and $215\text{--}220^\circ\text{C}$, 0.5 mbar for **1b**) to give the pure oxazaboroles **1a** (97%) and **1b** (93%), respectively, which were characterized by their NMR spectra.

(S)-1-Phenyl-3,3-diethylperhydropyrrolo[1,2-c][1,2,3]oxazaborole 1a.— $\delta_{\text{H}}(\text{CDCl}_3, 270 \text{ MHz})$ $7.71\text{--}7.76$ (m, 2H), $7.29\text{--}7.4$ (m, 3H), 3.64 (dd, J 5.5 , 9.7 , 1H), $3.45\text{--}3.55$ (m, 1H), $3.21\text{--}3.32$ (m, 1H), $1.38\text{--}2.0$ (m, 8H), 0.96 (t, 3H), 0.89 (t, 3H); $\delta_{\text{C}}(\text{CDCl}_3, 270 \text{ MHz})$ 134.1 , 129.6 , 127.4 , 84.5 , 71.8 , 43.0 , 31.8 , 28.1 , 27.5 , 26.8 .

(S)-1,3,3-Triphenylperhydropyrrolo[1,2-c][1,2,3]oxazaborole 1b.— $\delta_{\text{H}}(\text{CDCl}_3, 270 \text{ MHz})$ $7.9\text{--}8$ (m, 2H), $7.55\text{--}7.65$ (m, 2H), $7.1\text{--}7.5$ (m, 11H), 4.6 (dd, J 5.5 , 9.7 , 1H), $3.55\text{--}3.62$ (m, 1H), $3.28\text{--}3.37$ (m, 1H), $1.67\text{--}1.94$ (m, 3H), $0.86\text{--}0.98$ (m, 1H); $\delta_{\text{C}}(\text{CDCl}_3, 270 \text{ MHz})$ 147.3 , 143.8 , 134.6 , 130.3 , 128.1 , 127.8 , 127.7 , 127.6 , 127.1 , 126.7 , 126.4 , 126.3 , 87.7 , 74.3 , 43.7 , 29.9 , 27.5 . (These data are in good agreement with those given in ref. 25.)

2,2-Dimethylbutan-3-one (pinacolone = P, Alrich, 98%) was dried over K_2CO_3 and distilled under an argon atmosphere into Schlenk-flasks containing 4 \AA molecular sieves. THF (Riedel-de-Haën, +99.9%, stabilized with 2,6-di-*tert*-butyl-4-methylphenol) was dried over Na–K pearls and distilled under Ar. $\text{BH}_3\text{--THF}$ was either purchased (Aldrich, 1 mol dm^{-3} in THF, stabilized with $<0.005 \text{ mol dm}^{-3}$ NaBH_4) or synthesized according to literature procedures.^{18,19} The borane content of the solutions was determined in regular intervals by gas volumetry.²⁶

Acknowledgements

Financial support by the Bundesministerium für Bildung, Wissenschaft, Forschung und Technologie, grant nos. 03D0029B3 and 03D0029A0, and by the Fonds der Chemischen Industrie is gratefully acknowledged. We thank the Chemetall GmbH and the Degussa AG for generous gifts of chemicals.

References

- 1 S. Itsuno, K. Ito, A. Hirao and S. Nakahama, *J. Chem. Soc., Chem. Commun.*, 1983, 469.
- 2 E. J. Corey, R. K. Bakshi and S. Shibata, *J. Am. Chem. Soc.*, 1987, **109**, 5551.
- 3 E. J. Corey, R. K. Bakshi and S. Shibata, *J. Am. Chem. Soc.*, 1987, **109**, 7925.
- 4 L. Deloux and M. Srebink, *Chem. Rev.*, 1993, **93**, 763.
- 5 S. Wallbaum and J. Martens, *Tetrahedron: Asymmetry*, 1992, **3**, 1475.
- 6 J. G. Quallich, J. F. Blake and T. M. Woodall, *J. Am. Chem. Soc.*, 1994, **116**, 8516.
- 7 C. Franot, G. B. Stone, P. Engeli, C. Spöndlin and E. Waldvogel, *Tetrahedron: Asymmetry*, 1995, **6**, 2755.
- 8 D. J. Mathre, A. S. Thompson, A. W. Douglas, K. Hoogsteen, J. D. Carroll, E. G. Corley and E. J. J. Grabowski, *J. Org. Chem.*, 1993, **58**, 2880.
- 9 G. B. Stone, *Tetrahedron: Asymmetry*, 1994, **5**, 465.
- 10 A. W. Douglas, D. M. Tschäen, R. A. Reamer and Y.-J. Shi, *Tetrahedron: Asymmetry*, 1996, **7**, 1303.
- 11 E. J. Corey, M. Azimioara and S. Sarshar, *Tetrahedron Lett.*, 1992, **33**, 3429.
- 12 V. Nevalainen, *Tetrahedron: Asymmetry*, 1991, **2**, 1133.
- 13 V. Nevalainen, *Tetrahedron: Asymmetry*, 1994, **5**, 281.
- 14 L. P. Linney, C. R. Self and I. H. Williams, *J. Chem. Soc., Chem. Commun.*, 1994, 1651.
- 15 H. Jockel and R. Schmidt, *J. Chem. Soc., Perkin Trans. 2*, 1997, preceding paper.

- 16 J. R. Elliot, W. L. Roth, G. F. Roedel and E. M. Boldebuck, *J. Am. Chem. Soc.*, 1952, **74**, 5211.
- 17 B. Rice, J. A. Livasy and G. W. Schaeffer, *J. Am. Chem. Soc.*, 1955, **77**, 2750.
- 18 H. C. Brown, *Hydroboration*, W. A. Benjamin Inc., New York, 1962, p. 18.
- 19 G. F. Freeguard and L. H. Long, *Chem. Ind. (London)*, 1963, 471.
- 20 P. W. Atkins, *Physikalische Chemie*, VCH, Weinheim, 1987, p. 719.
- 21 H. C. Brown and B. C. S. Rao, *J. Am. Chem. Soc.*, 1960, **82**, 681.
- 22 J. D. Pasto and B. Lepeska, *J. Am. Chem. Soc.*, 1976, **98**, 1091.
- 23 J. Polster, *Reaktionskinetische Auswertung spektroskopischer Meßdaten*, Vieweg, Braunschweig, 1995, p. 76.
- 24 D. Enders, H. Kipphardt, P. Gerdes, L. J. Breña-Valle and V. Bhushan, *Bull. Soc. Chim. Belg.*, 1988, **97**, 691.
- 25 D. J. Mathre, T. K. Jones, L. C. Xavier, T. J. Blacklock, R. A. Reamer, J. J. Mohan, E. T. T. Jones, K. Hoogsteen, M. W. Baum and E. J. J. Grabowski, *J. Org. Chem.*, 1991, **56**, 751.
- 26 H. C. Brown, *Organic Synthesis via Boranes*, Wiley, New York, 1974, p. 241.

Paper 7/03700G
Received 28th May 1997
Accepted 27th August 1997